

## Reliable contacts to two-dimensional conduction layers

Victor Souw,<sup>a)</sup> Shi Li, and M. McElfresh

*Department of Physics, Purdue University, West Lafayette, Indiana 47907*

Zhan Duan, D. McInturff, and Aristo Yulius

*School of Electrical and Computer Engineering, Purdue University, West Lafayette, Indiana 47907*

E.-H. Chen and J. M. Woodall

*Department of Electrical Engineering, Yale University, New Haven, Connecticut 06520*

(Received 20 January 2000; accepted for publication 5 April 2000)

For many experiments and device applications, electrical contacts to a two-dimensional conduction layer must remain reliable under repeated temperature cycling between 300 and 77 K or lower. This work introduces the use of a silicon-doped InAs contact to the AlGaAs/GaAs two-dimensional electron gas which demonstrates exceptional reliability under such temperature cycling. The noise spectrum of AlGaAs/GaAs contacted with silicon-doped InAs shows almost no dependence on bias current; this fact can be used to improve the performance of device applications such as Hall sensors. In addition, this work introduces an alternative two-dimensional conduction structure, highly mismatched InAs/GaP. InAs/GaP contacted with Ti/Au shows reliability equal to AlGaAs/GaAs contacted with silicon-doped InAs. The InAs/GaP material may be more desirable for some applications because of the lower temperature dependence of its electronic properties and potentially easier integration with silicon-based microelectronics. © 2000 American Institute of Physics. [S0003-6951(00)04822-1]

The AlGaAs/GaAs two-dimensional electron gas (2DEG) has been instrumental in studies of quantum wells, quantum wires, quantum dots, and the integral and fractional quantum Hall effects.<sup>1-4</sup> In addition, the high mobility and well-defined conducting channel of this 2DEG make it a promising candidate for device applications such as high speed transistors<sup>5</sup> and Hall sensors.<sup>6-8</sup> Microscopic Hall sensor arrays based on the AlGaAs/GaAs 2DEG have been used, for instance, to study vortex dynamics in superconductors on the micron scale.<sup>9-15</sup> Since some applications require operation at temperatures below 77 K, reliability under repeated temperature cycling is essential, and low temperature dependence of electronic properties is very desirable.

However, during experiments with microscopic Hall sensor arrays based on the AlGaAs/GaAs 2DEG, the commonly used alloyed NiGeAu contact was observed to fail frequently, sometimes after only two or three temperature cycles. This high failure rate was observed in devices manufactured in two different laboratories. In order to improve reliability, this work introduces a new Si-doped InAs (InAs:Si) contact for AlGaAs/GaAs.

In addition, this work introduces highly mismatched InAs/GaP with Ti/Au contacts as a new material for microscopic Hall sensor arrays and other types of devices. Ti/Au-contacted InAs/GaP is very reliable, and the electronic properties of InAs/GaP show much smaller temperature dependence than those of AlGaAs/GaAs. InAs/GaP may also be more suitable for integration with existing microelectronics because of the better compatibility between GaP and Si.

Figure 1(a) shows the material structure of AlGaAs/GaAs with InAs:Si contacts. An undoped *i*-GaAs buffer layer is first grown on a GaAs substrate, followed by an *i*-Al<sub>0.3</sub>Ga<sub>0.7</sub>As spacer layer. The thin (20 Å) *i*-Al<sub>0.3</sub>Ga<sub>0.7</sub>As

spacer layer functions to suppress Shubnikov-de Haas oscillations by reducing the mobility of the 2DEG. Then, an *n*-Al<sub>0.3</sub>Ga<sub>0.7</sub>As layer and an *n*<sup>+</sup>-GaAs cap layer are grown. Finally, InAs:Si and Ti/Au layers are added.

During a 30 s anneal at 750 °C, Si from the InAs:Si layer diffuses into the AlGaAs layer, thus providing contact to the 2DEG. SIMS analysis shows no intermixing between the InAs:Si and GaAs; thus the dominant surface defect structure should remain unaffected by the anneal.<sup>16</sup> Moreover, since the bulk defect density of AlGaAs is significantly smaller than the density of diffused silicon, the electrical properties of the structure are expected to remain unaffected by the anneal.<sup>16</sup> The time and temperature of the anneal were opti-

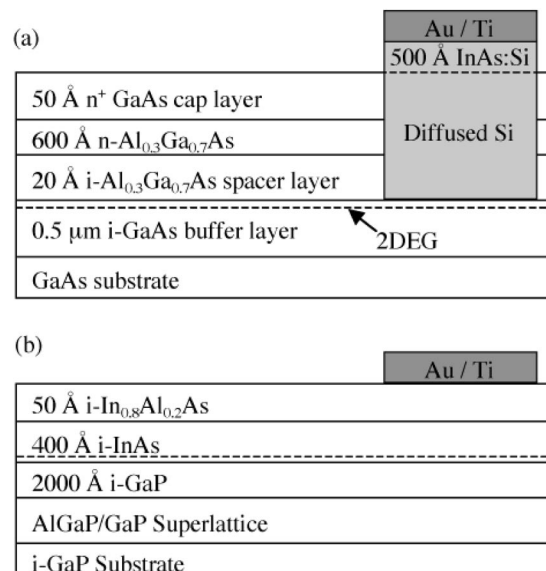


FIG. 1. Schematic of (a) AlGaAs/GaAs 2DEG structure with InAs:Si contacts and (b) InAs/GaP structure with Au/Ti contacts.

<sup>a)</sup>Electronic mail: vks@physics.purdue.edu

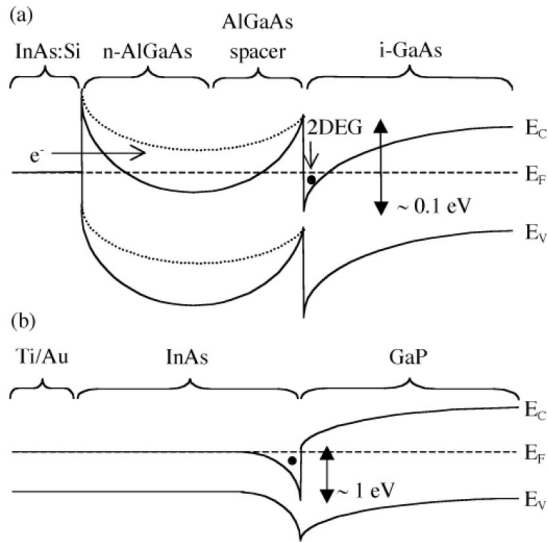


FIG. 2. (a) Energy band diagram for AlGaAs/GaAs 2DEG. The dotted line indicates the energy band without the InAs:Si contact. Note the increased band bending with the InAs:Si contact which shortens barrier width for tunneling into the 2DEG; (b) energy band diagram for InAs/GaP.

mized to produce the highest yield of ohmic contacts, the lowest contact resistance and the lowest temperature dependence of contact resistance. Previous studies of Si diffusion into GaAs have measured the diffusion depth of Si to be 700 Å at these annealing conditions.<sup>16</sup>

Figure 1(b) shows the highly mismatched InAs/GaP structure. On top of the *i*-GaP substrate, a 20 period superlattice consisting of 5 nm alternating layers of GaP and AlP is grown in order to prevent outdiffusion of any impurities from the substrate. Next, an intrinsic GaP layer, an intrinsic InAs layer, and an intrinsic  $\text{In}_{0.8}\text{Al}_{0.2}\text{As}$  cap layer are grown. The highly mismatched InAs/GaP interface gives rise to a high density ( $n \sim 10^{13} \text{ cm}^{-2}$ ) of ordered  $90^\circ$  dislocations, which are hypothesized to act as an array of structural dopants and to create a two-dimensional conduction channel at the interface.<sup>17,18</sup> Contact to this channel is made through the InAs by Ti/Au on the surface of the structure.

Figure 2(a) illustrates the InAs:Si electrical contact to the 2DEG in terms of the energy band diagram of AlGaAs/GaAs.<sup>19</sup> Silicon diffusion from the InAs:Si layer into the underlying AlGaAs layer results in band bending in the AlGaAs. This reduces the width of the potential barrier for electron tunneling. Figure 2(b) shows the band diagram of InAs/GaP.<sup>17</sup> Since no tunnel barrier exists in InAs/GaP, electrical contact to the interface layer is accomplished directly through the InAs epilayer.

Both structures were photolithographically patterned into Hall array devices containing a series array of 14 Hall sensors. Measurements of the Hall voltage versus applied magnetic field,  $V(H)$ , up to  $H=1$  T were conducted in a Quantum Design PPMS with a 7-T superconducting magnet. Each device was repeatedly cycled between 77 and 300 K, with  $V(H)$  measurements taken during each cycle at  $T=77$  K and  $T=300$  K. A bias current of 30  $\mu\text{A}$  was applied as an ac square wave in order to cancel electrical asymmetries. Noise voltage spectra were measured using a Stanford Research 850 digital lock-in amplifier.

Table I summarizes the electrical characteristics of the two materials. In the case of InAs:Si-contacted AlGaAs/

TABLE I. Electrical characteristics of the AlGaAs/GaAs 2DEG and InAs/GaP structures.

	AlGaAs/GaAs 2DEG		InAs/GaP	
	300 K	77 K	300 K	77 K
Sheet density ( $10^{11} \text{ cm}^{-2}$ )	12	8.7	70	60
Mobility ( $\text{cm}^2/\text{V s}$ )	6300	28 000	800	730
Magnetic sensitivity ( $\Omega/\text{T}$ )	600	840	520	590
Magnetic hysteresis (mT)	4.5	0.1	0.34	0.10

GaAs, decreasing the temperature from 300 to 77 K results in a 28% decrease in sheet carrier concentration and a 340% increase in mobility. The measured magnetic field sensitivity, defined as the Hall voltage divided by the bias current and applied magnetic field, increases by 40% at 77 vs 300 K.

The practical limit for magnetic field sensitivity is the magnetic field hysteresis, a small difference between the  $V(H)$  measured in increasing and decreasing magnetic field. The hysteresis is not caused by irreproducibilities in temperature or applied magnetic field since different Hall elements on each device can show different amounts of hysteresis. At 300 K, the hysteresis is equivalent to as much as 4.5 mT; that decreases by 98% to only 0.1 mT at 77 K. After 20 temperature cycles between 300 and 5 K, none of the 30 contacts failed, and the magnetic field sensitivity changed by less than 0.4%, thus demonstrating excellent reliability under temperature cycling. By comparison, an AlGaAs/GaAs device with alloyed NiGeAu contacts showed that five of the 30 contacts had failed within 20 temperature cycles, a failure rate typical in our experience with alloyed NiGeAu contacts.

In Ti/Au-contacted InAs/GaP, decreasing the temperature from 300 to 77 K results in a 14% decrease in sheet carrier concentration,<sup>20,21</sup> an 8.8% decrease in mobility and a 14% increase in magnetic field sensitivity. Note that the temperature dependence of all three quantities is significantly lower than in AlGaAs/GaAs. The magnetic field sensitivity of InAs/GaP is also lower than that of AlGaAs/GaAs: 13% lower at 300 K and 30% lower at 77 K. The magnetic field hysteresis in InAs/GaP is only 0.34 mT at 300 K, significantly lower than in AlGaAs/GaAs at 300 K, and 0.1 mT at 77 K, equal to that of AlGaAs/GaAs. Twenty temperature cycles between 300 and 5 K resulted in no contact failures and less than 0.4% change in magnetic field sensitivity. Hence, Ti/Au contacted InAs/GaP shows reliability equal to that of InAs:Si-contacted AlGaAs/GaAs.

Figure 3 shows the noise spectra of the two types of devices. At zero bias current, the noise spectra of both devices are identical. Below 10 Hz, the noise voltage decreases very rapidly from approximately  $500 \text{ nV}/\sqrt{\text{Hz}}$  to less than  $25 \text{ nV}/\sqrt{\text{Hz}}$ , but above 10 Hz, the noise voltage is approximately independent of frequency.

Increasing the bias current results in increased noise voltage, mostly at frequencies above 3 Hz. As the current is increased from 0 to 40  $\mu\text{A}$ , the average noise between 20 and 50 Hz increases from 13 to 30  $\text{nV}/\sqrt{\text{Hz}}$  in the InAs:Si-contacted AlGaAs/GaAs device. In contrast, it increases

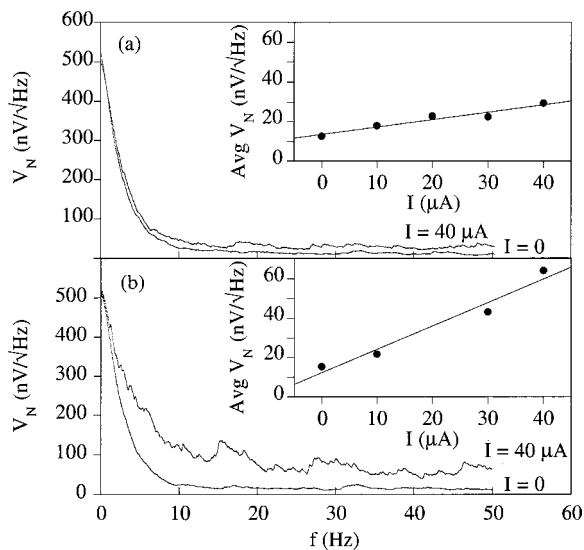


FIG. 3. The square root of the voltage noise spectral density ( $V_N$ ) as a function of frequency and applied bias current at 300 K. The inset shows the dependence of the average noise between 20–50 Hz on the applied bias current; (a) AlGaAs/GaAs; (b) InAs/GaP.

from 15 to 64  $\text{nV}/\sqrt{\text{Hz}}$  in the Ti/Au-contacted InAs/GaP device. Thus, at a bias current of 40  $\mu\text{A}$ , the AlGaAs/GaAs device with InAs:Si contacts shows a 54% lower noise level than the InAs/GaP device with Ti/Au contacts.

The relatively small temperature dependence observed in the InAs/GaP material is consistent with carrier generation by the interface defect structure. Since the magnetic sensitivity  $= V_H/IH = 1/n_s e$ , the smaller magnetic sensitivity of InAs/GaP can likely be attributed to the higher sheet carrier concentration compared to AlGaAs/GaAs.

The larger average noise voltage in InAs/GaP may be related indirectly to its lower mobility and therefore higher resistance ( $R \propto 1/\mu n_s$ ). It is in fact observed that the average noise level depends only on the square root of the device resistance, regardless of the material. This suggests that thermal noise ( $V_N = \sqrt{4kTR}$ ) is the dominant contribution to the measured noise voltage.

The high mobility of AlGaAs/GaAs makes it particularly suitable for application in Hall sensors operated in constant-voltage or constant-power mode, where the magnetic field sensitivity is proportional to the mobility.<sup>22</sup> In principle, this sensitivity can be improved further by increasing the mobility, but at very high mobilities and magnetic fields, AlGaAs/GaAs may become unsuitable as a magnetic field sensor because of Shubnikov–de Haas oscillations and the integral quantum Hall effect. However, since the noise voltage depends only weakly on the bias current, while the Hall voltage increases linearly with current, it is possible to further improve the signal-to-noise ratio by applying higher bias currents. AlGaAs/GaAs is therefore particularly desirable for its high magnetic field sensitivity.

In contrast, the lower mobility of InAs/GaP favors operation in constant-current mode, where the sensitivity is independent of mobility.<sup>22</sup> Nevertheless, InAs/GaP shows up to 30% smaller magnetic field sensitivity than AlGaAs/GaAs. Furthermore, unlike in AlGaAs/GaAs, the stronger current dependence of the noise voltage suggests that this sensitivity cannot be improved by applying larger bias currents.

Although AlGaAs/GaAs demonstrates higher magnetic field sensitivity, the appreciable temperature dependence of this sensitivity can lead to significant errors in magnetic field measurement if the operating temperature is not well controlled. Furthermore, the large magnetic field hysteresis observed near  $T=300$  K limits the accuracy of the AlGaAs/GaAs Hall sensors near room temperature.

In contrast, the relatively low temperature dependence observed in the InAs/GaP Hall sensors makes them especially suitable for magnetic field measurements when the operating temperature varies or is not well controlled. In addition, the relatively low magnetic field hysteresis near 300 K enables measurements near room temperature.

In conclusion, this work demonstrates the suitability of InAs:Si-contacted AlGaAs/GaAs and Ti/Au-contacted InAs/GaP for low- and variable-temperature device applications. The new InAs:Si contact enables the use of AlGaAs/GaAs in applications which require robustness under repeated temperature cycling, and the noise characteristics of this structure can be exploited to further improve the signal-to-noise ratio. In addition, InAs/GaP with Ti/Au contacts demonstrates reliability equal to AlGaAs/GaAs with InAs:Si contacts and also offers more uniform electrical properties over a wider temperature range.

<sup>1</sup> *Interfaces, Quantum Wells and Superlattices*, edited by C. R. Leavens and R. Taylor (Plenum, New York, 1987).

<sup>2</sup> *Science and Engineering of One- and Zero-Dimensional Semiconductors*, edited by S. P. Beaumont and C. M. Sotomayor Torres (Plenum, New York, 1989).

<sup>3</sup> K. von Klitzing, G. Dorda, and M. Pepper, *Phys. Rev. Lett.* **45**, 494 (1980).

<sup>4</sup> D. C. Tsui, H. L. Stormer, and A. C. Gossard, *Phys. Rev. Lett.* **48**, 1559 (1982).

<sup>5</sup> J. Pozela, *Physics of High-Speed Transistors* (Plenum, New York, 1993).

<sup>6</sup> P. Kleinschmidt and F. Schmidt, *Sens. Actuators A* **31**, 35 (1992).

<sup>7</sup> S. Kawahito, S. O. Choi, M. Ishida, and T. Nakamura, *Sens. Actuators A* **40**, 141 (1995).

<sup>8</sup> R. S. Popovic, J. A. Flanagan, and P. A. Besse, *Sens. Actuators A* **56**, 39 (1996).

<sup>9</sup> Y. Abulafia, M. McElfresh, A. Shaulov, Y. Yeshurun, Y. Paltiel, D. Majer, H. Shtrikman, and E. Zeldov, *J. Appl. Phys.* **72**, 5471 (1999).

<sup>10</sup> Y. Abulafia, Y. Wolfus, M. McElfresh, A. Shaulov, Y. Yeshurun, Y. Paltiel, H. Shtrikman, and E. Zeldov, *J. Appl. Phys.* **85**, 2891 (1998).

<sup>11</sup> S. Berry, M. Konczykowski, P. H. Kes, and E. Zeldov, *Physica C* **282-287**, 2259 (1997).

<sup>12</sup> Y. Abulafia, D. Giller, Y. Wolfus, A. Shaulov, Y. Yeshurun, D. Majer, E. Zeldov, J. L. Pang, and R. L. Greene, *J. Appl. Phys.* **81**, 4944 (1997).

<sup>13</sup> D. Majer, E. Zeldov, M. Konczykowski, V. B. Geshkenbein, A. I. Larkin, L. Burlachkov, V. M. Vinokur, and N. Chikumoto, *Physica C* **235-240**, 2765 (1994).

<sup>14</sup> B. Khaykovich, E. Zeldov, M. Konczykowski, D. Majer, A. I. Larkin, and J. R. Clem, *Physica C* **235-240**, 2757 (1994).

<sup>15</sup> M. Konczykowski, D. Majer, E. Zeldov, N. Chikumoto, and V. M. Vinokur, *Physica C* **235-240**, 2965 (1994).

<sup>16</sup> A. Yulius, Thesis, Purdue University, 1998.

<sup>17</sup> V. Gopal, E. P. Kvam, T. P. Chen, and J. M. Woodall, *Appl. Phys. Lett.* **72**, 2319 (1998).

<sup>18</sup> V. Gopal, E.-H. Chen, E. P. Kvam, and J. M. Woodall, *J. Vac. Sci. Technol. B* **17**, 1767 (1999).

<sup>19</sup> M. R. Melloch, *Thin Solid Films* **231**, 74 (1993).

<sup>20</sup> The extraction of sheet carrier concentration and mobility in InAs/GaP is complicated by the presence of multiple conduction channels (e.g., the two-dimensional interface layer and the bulk InAs). Table I shows the apparent sheet carrier concentration and mobility.

<sup>21</sup> V. Gopal, V. Souw, E.-H. Chen, E. P. Kvam, M. McElfresh, and J. M. Woodall, *J. Appl. Phys.* **87**, 1350 (2000).

<sup>22</sup> R. S. Popovic, *Hall Effect Devices-Magnetic Sensors and Characterization of Semiconductors* (Adam Hilger, London, 1995).